Comparison of Pyrolysis Liquids from Continuous and Batch Biochar Production—Influence of Feedstock Evidenced by FTICR MS

energies

MDPI

Article

Comparison of Pyrolysis Liquids from Continuous and Batch Biochar Production—Influence of Feedstock Evidenced by FTICR MS

Wolfram Buss [1,2,*,†], Jasmine Hertzog [3,*,†], Julian Pietrzyk [1], Vincent Carré [3], C. Logan Mackay [4], Frédéric Aubriet [3] and Ondřej Mašek [1,*]

1 UK Biochar Research Centre, School of GeoSciences, University of Edinburgh, Crew Building, Alexander Crum, Brown Road, Edinburgh EH9 3FF, UK; julian.pietrzyk@mialgae.com
2 Research School of Biology, Australian National University, 134 Linnaeus Way, Canberra 2601, Australia
3 LCP-A2MC, FR 2843 Institut Jean Barriol de Chimie et Physique Moléculaires et Biomoléculaires, FR 3624 Réseau National de Spectrométrie de Masse FT-ICR à très Haut Champ, Université de Lorraine, ICPM, 1 Boulevard Arago, CEDEX 03, 57078 Metz, France; vincent.carre@univ-lorraine.fr (V.C.); frederic.aubriet@univ-lorraine.fr (F.A.)
4 SIRCAMS, School of Chemistry, University of Edinburgh, Edinburgh EH9 3FJ, UK; lmackay@ed.ac.uk
* Correspondence: wolfram.buss@anu.edu.au (W.B.); jasmine.hertzog@univ-rouen.fr (J.H.); ondrej.masek@ed.ac.uk (O.M.)
† Equal contributing authors.

Abstract: Bio-oils from biomass pyrolysis can be a resource for upgrading to chemicals or fuels. Here, for the first time, we compare the composition of bio-oils produced from two feedstocks (wheat straw, softwood) in pyrolysis units of different mode of operation (continuous—rotary kiln vs. batch) using Fourier transform ion cyclotron resonance mass spectrometry (FTICR MS) in different ionization modes (APPI (+), ESI (+/−)). Our results demonstrate that the pyrolysis unit design had only a minor influence on the composition of bio-oils produced from low-mineral containing wood biomass. Yet, the wheat straw-derived bio-oil produced in the continuous unit comprised lower molecular weight compounds with fewer oxygen-containing functional groups and lower O/C and H/C ratios, compared to bio-oils from batch pyrolysis. Longer residence time of vapours in the heated zone in the rotary kiln and a higher mineral content in wheat straw resulted in increased catalytically-mediated secondary reactions that favoured further bio-oil decomposition. This work shows for the first time that it is possible to produce distinct bio-oils without the need for external catalyst addition, by matching reactor type/design and feedstock.

Keywords: pyrolysis; bio-oil; complex mixtures; FTICR MS; biochar

Citation: Buss, W.; Hertzog, J.; Pietrzyk, J.; Carré, V.; Mackay, C.L.; Aubriet, F.; Mašek, O. Comparison of Pyrolysis Liquids from Continuous and Batch Biochar Production—Influence of Feedstock Evidenced by FTICR MS. *Energies* **2021**, *14*, 9. https://dx.doi.org/10.3390/en14010009

Received: 10 November 2020
Accepted: 18 December 2020
Published: 22 December 2020

1. Introduction

The transition to a circular economy brings resource re-use, recycling and recovery to the forefront of political agendas globally [1–3]. The concept of a circular economy can be applied to all areas of the economy, including agricultural and forestry where biomass residues are often left in the field or are burned with the plant-derived carbon stored in the biomass being released back into the atmosphere [4]. A promising way for biomass upgrading is pyrolysis that converts the material into non-condensable gas, liquid, and solid residue. Operating parameters, such as residence time, heating rate, and temperature, control the product yield in each fraction and define slow, fast, and flash pyrolysis [5,6].

Slow pyrolysis is the process of heating biomass under oxygen limited conditions typically at temperatures between 300 and 700 °C with a residence time of the biomass in the heated zone of around 5–30 min (in the rotary kilns) [7]. Of the three different pyrolysis techniques, it results in the highest yield of pyrolysis solids (20–40 wt %) with liquid and gas yields of 20–40 wt % and 10–25 wt %, respectively [8]. When used for environmental

management the solid pyrolysis fraction is called biochar [9]. Biochar contains aromatic carbon that is very stable against chemical and biological degradation, therefore, it is proposed as a negative emission technology [10,11].

There has been a surge in research into the uses and benefits of biochar, which spans from increasing plant available water content in soil to soil remediation and non-soil uses, such as energy storage [9,12–14]. Yet, the released pyrolysis gases and liquids are typically burned in many commercial pyrolysis units [7]. Crombie and Mašek (2014) demonstrated that a slow pyrolysis system focused on biochar production from agricultural and forestry residues can be sustained based on the energy content in the gases alone [15]. Using electric energy generated from renewable sources could make the use of the biomass itself to kickstart the pyrolysis process fully obsolete. This would free-up the pyrolysis liquids as a valuable resource, e.g., for upgrading to liquid fuels [16].

The liquid fraction from biomass pyrolysis, also called bio-oil, is a highly complex mixture comprising thousands of chemical species covering a wide range of mass and polarity [17–19]. Bio-oils have higher water and oxygen contents than liquid fossil fuels, which prevents the direct use as fuel [20,21]. Therefore, upgrading deoxygenation treatments are necessary. Thorough molecular description of bio-oils is essential in order to improve both the conversion and upgrading processes. In this regard, non-targeted analysis using ultra-high-resolution mass spectrometry, combined with complementary ionization sources, has proven its efficiency [22].

The most powerful technique, in terms of mass accuracy and resolving power, is Fourier-transform ion cyclotron resonance mass spectrometry (FTICR MS). Electrospray ionization (ESI) analysis is the most commonly employed source for bio-oil characterization [22], which typically does not ionize the less polar to non-polar bio-oil components. These can instead be analysed with laser desorption ionization (LDI) or atmospheric pressure photoionization (APPI). In previous studies, it was demonstrated that these complementary ionization sources ensured a comprehensive molecular bio-oil composition description and could be used to assess the efficiency of different catalytic treatments [19,23]. Moreover, positive and negative detection modes were also shown to be complementary for the characterisation of bio-oils [24].

Recently, we were able to show that biochars from different pyrolysis units (continuous vs. batch) do not differ significantly in the volatile matter content, a key physicochemical biochar property [25]. Here, we investigate the effects of pyrolysis unit design, nature of feedstock, and temperature on the pyrolysis liquids composition. The aim was to determine whether and to what extent the composition of pyrolysis liquids changes between different units that produce comparable biochar. Such understanding is important for selection and design of efficient biochar production technology that maximises carbon sequestration as well as production of value-added liquid co-products with minimum negative environmental impacts. With one of the overarching goals being upgrading as a fuel.

In this study, ESI (+/−) and APPI (+) FTICR MS was used to analyse pyrolysis liquids from two lignocellulosic feedstocks (softwood pellets (SWP) and wheat straw pellets (WSP)), at two pyrolysis temperatures (550 and 700 °C) and in two pyrolysis units of different type and scale (small-scale batch unit vs. pilot-scale continuous unit). If the liquid composition differs due to the pyrolysis mode of operation, it likely only differs marginally, which is unlikely detected by conventional techniques. FTICR MS does not only give us a thorough characterisation of the chemical composition, it also helps us to understand the mechanisms that resulted in the differences in composition according to the different pyrolysis conditions.

2. Materials and Methods

2.1. Pyrolysis

2.1.1. Feedstocks

The feedstocks used in this study were softwood pellets (SWP) consisting of pine and spruce, and wheat straw pellets (WSP). The feedstocks were characterised by proximate analysis (thermogravimetric analysis) and ultimate analysis (CHN) as described in Crombie et al. [26]. The compositions of the feedstocks are shown in Table 1. The feedstocks were used for pyrolysis as received, without any additional pre-processing.

Table 1. Biomass feedstock composition. Mean values and standard deviations for five replicates are provided.

Feedstock	Moisture	Volatile Matter	Fixed C	ash	C	H	N	Bulk Density	Diameter	Length
	wt%, a.r	wt%, d.b.	wt%, d.b.	wt%, d.b.	wt%, d.b.	wt%, d.b.	wt%, d.b.	g cm^{-3}	mm	mm
softwood pellets (SWP)	6.71 ± 0.03	77.92 ± 0.44	14.22 ± 0.38	1.07 ± 0.12	49.95 ± 0. 01	6.65 ± 0.06	<0.1	0.7	6	14 ± 4
wheat straw (WSP)	7.22 ± 0.22	70.12 ± 0.55	15.29 ± 1.08	6.44 ± 0.28	45.16 ± 0. 05	5.44 ± 0.01	0.58 ± 0.01	0.5	6	18 ± 4

2.1.2. Batch Slow Pyrolysis in a Fixed-Bed Quartz Tube

The batch slow pyrolysis unit (UKBRC Stage I) is a fixed-bed reactor comprising a quartz glass reactor tube (50 mm inner diameter) with a sintered glass frit at the centre [26]. The reactor tube is heated by a 12-kW infrared image furnace (ULVAC RHL-P610C, ULVAC, Methuen, MA, USA, with temperature control based on a thermocouple immersed within the test sample.

The biomass sample (~50 g) was charged to the reactor tube before assembling the pyrolysis unit and condensation train (Section 2.1.4). The reactor was pre-purged with nitrogen that was then also used as an inert carrier gas passing through the sample bed at a steady flow rate of 0.33 L.min^{-1}, corresponding to a linear cold flow velocity within the empty reactor tube of 3 mm s^{-1}. Heating rate and residence time at highest treatment temperature were selected to match the conditions in the continuous pyrolysis unit (UKBRC Stage III) shown in Table 1.

Table 1. Key characteristics of bio-oils production. All pyrolysis with the Stage I unit were performed in duplicates represented by '-1′ and '-2′. HTT, highest treatment temperature; SWP, softwood pellets; WSP, wheat straw pellets.

Name	HTT	Heating Rate	Residence Time at HTT	Feedstock	Pyrolysis Unit	Biochar Yield	Bio-Oil Yield
	°C	°C·min^{-1}	min			wt%, d.b.	wt%, d.b.
SWP550-1	550	80	10	SWP	Stage I–batch	20.4	46.6
SWP550-2	550	80	10	SWP	Stage I–batch	22.3	47.1
SWP700-1	700	87	10	SWP	Stage I–batch	18.0	46.3
SWP700-2	700	87	10	SWP	Stage I–batch	18.1	45.3
WSP550-1	550	80	5	WSP	Stage I–batch	25.3	44.1
WSP550-2	550	80	5	WSP	Stage I–batch	25.8	44.6
WSP700-1	700	80	6	WSP	Stage I–batch	21.8	43.7
WSP700-2	700	80	6	WSP	Stage I–batch	23.4	42.6
SWP550-III	550	~80	~10	SWP	Stage III–continuous	24.0	37.0
WSP550-III	550	~80	~5	WSP	Stage III–continuous	26.0	43.0

Sample temperature, reactor pressure and differential pressures were monitored and logged within the pyrolysis unit. In Table 1, the solid and liquid product yields are given expressed as weight percent on dry feedstock basis. The handling losses of solids and liquid products were estimated at 5–10% in total.

2.1.3. Continuous Slow Pyrolysis in Rotary Kiln

Detailed description of the UKBRC Stage III Pyrolysis Unit and its operation can be found in Masek et al. (2018) [25]. The unit consists of a sealed stainless-steel rotary drum (ID = 0.244 m, heated length 2.8 m), and is heated by three sets of electrical heaters with combined rating of 50 kW. During operation, the biomass moves through the rotary drum purged by nitrogen as an inert carrier gas. After separation of pyrolysis vapours and solids, the solids (biochar) are transported by a conveyor belt into a sealed metal drum while the gases and vapours are burned in an afterburner.

The residence time at HTT within the continuous unit was determined based on the mean residence time of the feedstock in the reactor as measured using differently coloured feedstock pellets in a cold run (no heating of the unit). To calculate the heating rate, in addition to the residence time, the temperature profile was measured using five thermocouples along the length of the reactor (in the bed of moving pellets). From this, we knew at what point in the kiln the pellets reached the peak temperature and the average heating rate was calculated. The reason for different residence times of the feedstocks is the different movement of pellets through the reactor due to different particle size and density, but also different temperature profile due to different composition of the biomass. The heating rates and residence times at HTT were replicated with the batch unit.

To collect the gas and pyrolysis samples for this work, a small proportion of the vapour stream was continuously withdrawn, at approx. 1 L.min^{-1}, during steady state operation, and passed through a condensation train.

2.1.4. Condensation Train for Pyrolysis Liquid Recovery

The train consisted of two parts: first the gas passed through a thimble filter heated to 170 $\pm$ 15 °C where any entrained particulates were separated, as well as some of the heavy tars. Second, the particulate-free gas passed through a condenser at ambient-temperature followed by two cold traps maintained at $-$50 to $-$30 °C using liquid nitrogen-cooled acetone.

2.2. Fourier Transform Ion Cyclotron Resonance Mass Spectrometry (FTICR MS)

Bio-oil characterization was performed using a 12 T SolariX FTICR (Bruker Daltonics, Bremen, Germany) unit equipped with ESI and APPI sources (Bruker Daltonics, Bremen, Germany). The operating parameters and ionization methods were optimized by using FTMS Control software (V2.1.0, build 98, Bruker Daltonics, Bremen, Germany).

2.2.1. Electrospray Ionization (ESI) FTICR MS

For ESI FTICR MS analyses, bio-oil samples were diluted to a final concentration of 0.1% in methanol (Analytical grade; VWR—Prolabo). For ESI (+), 0.1 mg.mL^{-1} sodium acetate (Analytical grade; Fisher Scientific) was added to favour cationization [24].

Measurements were performed in both (+) and ($-$) ion modes. The capillary voltage was set at $\pm$ 4 kV and the end plate offset at –500 V. The source was tuned with nebulizer and dry gas (1–1.8 bar and 4–6 L.min^{-1}, respectively) and heated to 180 °C. The sample was directly infused in the source at a flow rate of 200 µL h^{-1}. The generated ions were accumulated for 0.3 s per scan and 200 scans were summed to achieve the final mass spectrum in the mass-to-charge ratio (m/z) range 129–700. The mass resolution was ~680,000 at m/z 400 with a transient length of 3 s.

2.2.2. Atmospheric Pressure Photoionization (APPI) FTICR MS

For the APPI analyses achieved in (+) mode, the softwood-based pyrolysis liquids were diluted in methanol to a final concentration of 0.1%. The wheat straw pyrolysis liquids were diluted to 1%. No dopants were added as successfully performed in the previous study [19].

The APPI source is equipped with a krypton lamp that emits 10.6 eV photons. The voltages of the capillary and end plate offset were set at 1000 V and $-$500V, respectively.

The source was tuned with nebulizer gas (1.8 bar) and dry gas (6 L.min^{-1}) and heated to 180 °C. The infusion flow rate was set to 1 mL.h^{-1}. Ions were accumulated for 0.05 s and a sum of 100 scans yielded the final mass spectrum that extended from m/z 129 to 1000. The length of the transient was 1.5 s and the mass resolution was ~340,000 at m/z 400 [19].

2.2.3. Data Post-Acquisition Treatment

The mass spectra recorded in ESI and APPI were calibrated and analysed with Data Analysis V4.4, build 102.47.2299 (Bruker Daltonics). The internal calibration was done with known oxygenated compounds specific to each analytical condition. Then peak lists of ions with a signal-to-noise ratio greater than 4 were generated and submitted to the software PetroOrg (Florida State University) for assignment. The attribution parameters were as following: $C_{1\text{-}100}H_{2\text{-}200}O_{0\text{-}20}N_{0\text{-}20}S_{0\text{-}1}$ and sodium adducts were considered for ESI (+) analyses. The tolerated mass error was set at ±1 ppm. CH, CHO, CHON, CHN, and CHOS compound families were identified. The molecular description achieved for the different samples with the different analytical conditions is given by the heteroatom class distribution (Table S1). Additionally, assignments were plotted on van Krevelen diagrams according to their O/C and H/C ratios. From this graph, it is possible to distinguish chemical compounds, according to their ratios, such as lipids (O/C < 0.2 and H/C ≈ 2), sugar derivatives (0.8 < O/C < 1 and H/C > 1.5) and pyrolytic lignin (0.2 < O/C < 0.6 and H/C ≈ 1) [27,28]. Sugar derivatives typically originate from the pyrolysis of cellulose and hemicellulose whereas lignin pyrolysis forms phenolics.

2.3. Statistical Analysis

Perseus software was used to achieve Principal Component Analysis (PCA) of the features from ESI (+/−) and APPI (+) FTICR MS analyses of the different samples. Profile searching was performed with the same software to extract specific features related to the clusters observed on the PCA. Then, the extracted contributions were plotted on van Krevelen diagrams (H/C vs. O/C and H/C vs. m/z) and according to their heteroatom classes.

3. Results

3.1. Pyrolysis Product Yields

In the continuous unit the biochar yield was slightly higher and the liquid yield lower compared to the batch unit (Table 1). Ronsse et al. (2013) reported comparable biochar yields to our results in straw biochar (25.4% at 600 °C and 23.0% at 750 °C, both with 10 min residence time), but slightly higher yields from the pyrolysis of woody feedstock (24.4% at 600 °C and 23.0% at 750 °C) [29]. Softwood pellet (SWP) feedstock resulted in a lower biochar yield and higher pyrolysis liquids yield compared to wheat straw pellets (WSP) likely due to a mineral/higher ash content in the WSP feedstock (1.07% SWP vs. 6.44% WSP; Table 1). Feedstock with higher mineral contents (both inherent and added ash) typically have higher biochar yields [30,31]. Alkali and alkaline earth metals in the ash catalyse biochar formation [32–34] and in addition, the ash comprises of inorganics that cannot be converted into pyrolysis vapours [31]. Both processes increase the solid fraction over the vapour (gas and liquid) fraction.

3.2. Molecular Description of the Bio-Oils According to the Different Analytical Conditions

We analysed the pyrolysis oils via FTICR using two complementary ionization sources. ESI enables differentiation into lipids, pyrolytic sugars, and lignin derivatives [19] mainly as polar compounds with acidic and basic functional groups [35]. ESI (+) is more specific to sugar-derivatives, characterized by a low level of saturation and high oxygen amounts [19]. ESI (−) is better suited for lignin derivatives with a greater diversity of compounds in terms of degree of unsaturation and number of oxygen atoms [19]. With APPI (+), less polar species, with lipids and pyrolytic lignin are observed [19]. APPI (+) typically enables detection of compounds with lower H/C ratios than ESI (+), higher m/z ratios [19] and

offers higher reproducibility than ESI, due to APPI's lower sensitivity towards ionization compounds, which can significantly affect the ionization process and subsequently biases the bio-oil analysis by ESI.

Figure 1 shows van Krevelen diagrams of the two pyrolysis oils produced at 700 °C with the Stage I unit. Each point corresponds to one CxHyOz assignment highlighting the bio-oil molecular complexity. The different ionisation modes pick up different chemical classes in the pyrolysis liquids with a variety of H/C and O/C ratios (Table S1, Figure 1) as previously shown [19,23,24].

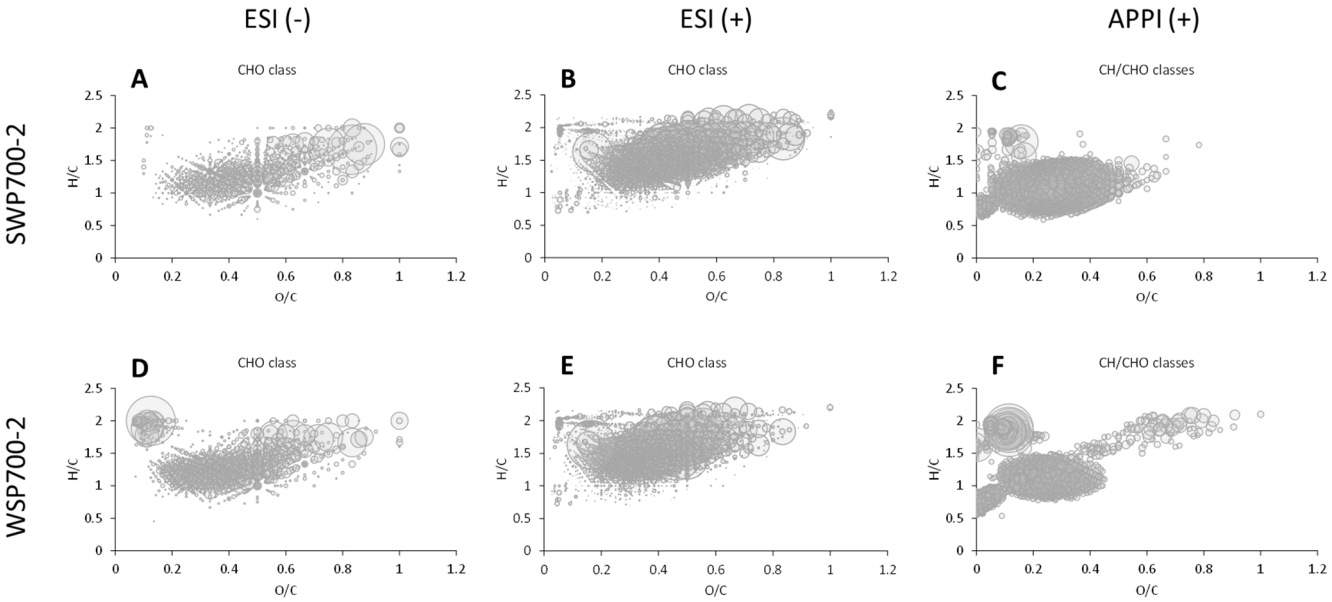

Figure 1. Van Krevelen diagrams of CxHyOz compounds assigned and detected by ESI (+/−) and APPI (+) FTICR MS in bio-oils from pyrolysis, at 700 °C, of soft wood pellets (SWP700-2) and wheat straw pellets (WSP700-2). (**A**) SWP in ESI (−); (**B**) SWP in ESI (+); (**C**) SWP in APPI (+); (**D**) WSP in ESI (−); (**E**) WSP in ESI (+); (**F**) WSP in APPI (+).

Table S1 demonstrates that the assigned bio-oil compounds contain oxygen for more than 95% of the features, independent of the analytical parameters. Among the CHO class, there are some lipids and pyrolytic lignin and sugar derivatives (Figure 1). More CHON and CHN species were detected in positive ion mode (ESI and APPI). Cole et al. (2013) proposed that the basicity of the N-species is responsible for their better detection in these ionization conditions [36]. They also reported a significant number of N-containing compounds in fast pyrolysis liquids produced from switchgrass straw. This latter fact is also observed in this study where the number of CHN and CHON assignments is higher in the WSP samples than in SWP (Table S1). This agrees with the elemental composition of the two feedstocks where the N content in straw is higher compared to softwood (Table 1).

Sulphur-containing species were only detected in ESI (−) as previously observed [24] and are likely sulfonated compounds from sulfonic acid derivates [28]. Some CHOB species were assigned, which were also identified via FTICR MS and ^{11}B NMR by Jarvis et al. (2014) [37]. The authors demonstrated that boron was part of polysaccharide complexes. Boron-polyol interactions, in the form of borate, are paramount to plant growth [38,39] and borate is detectable in negative-ion mode by ESI FTICR MS [40,41].

The pyrolysis temperature (550 °C vs. 700 °C) did not have an apparent effect on the bio-oil compositions in either of the feedstocks. In the PCA plots generated from the data obtained by the different analysis techniques, the replicates produced under the same conditions show similar variability as the liquids produced under different temperatures (Figures 2–4).

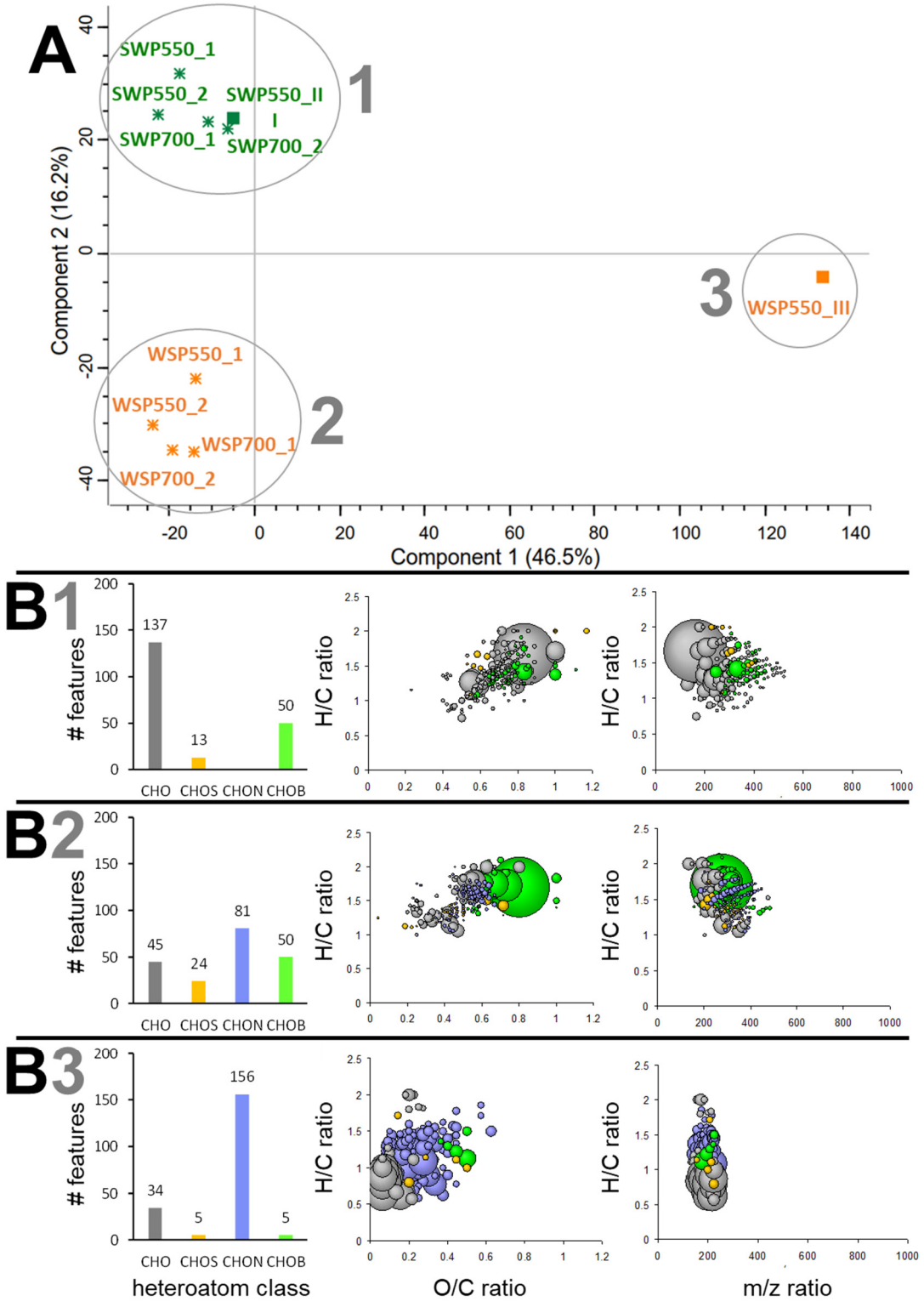

Figure 2. (**A**) Principal component analysis (PCA) score plot of all m/z features from bio-oils measured by ESI (−) FTICR MS. Wheat straw pellets-derived bio-oils in orange, softwood pellets bio-oils in green, small-scale unit bio-oils highlighted by a star and pilot-scale bio-oils by a full square. (**B**) Two hundred features specific to group 1, 2 and 3 observed in panel (**A**) were extracted and represented as (from left to right) bar chart according to their heteroatom classes, van Krevelen diagram (O/C vs. H/C) and m/z vs. H/C-ratios. The bubble size is relative to peak intensity.

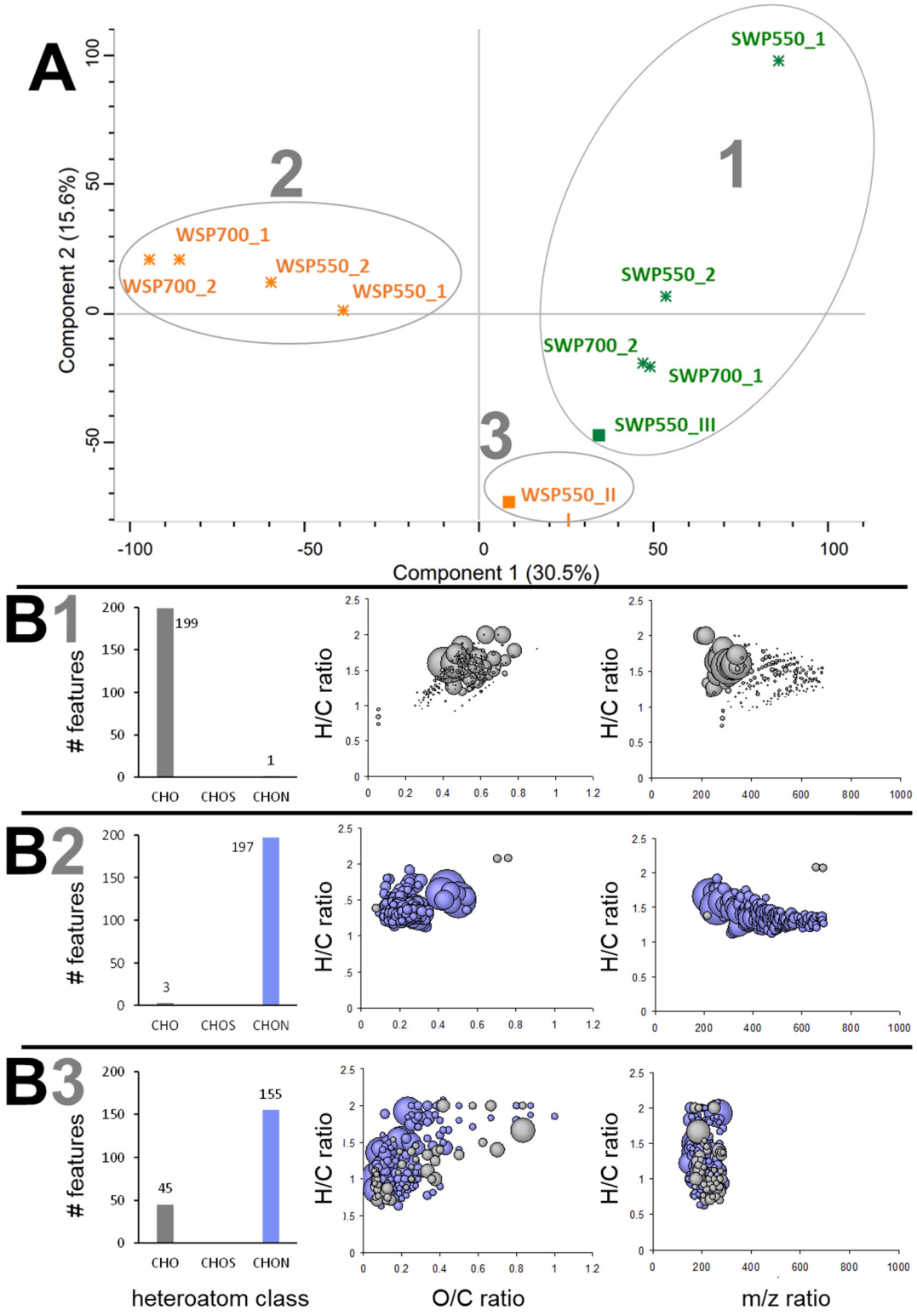

Figure 3. (**A**) Principal component analysis (PCA) score plot of all m/z features from bio-oils measured by ESI (+) FTICR MS. Wheat straw pellets-derived bio-oils in orange, softwood pellets bio-oils in green, small-scale unit bio-oils highlighted by a star and pilot-scale bio-oils by a full square. (**B**) Two hundred features specific to group 1, 2 and 3 observed in panel (**A**) were extracted and represented as (from left to right) bar chart according to their heteroatom classes, van Krevelen diagram (O/C vs. H/C) and m/z vs. H/C-ratios. The bubble size is relative to peak intensity.

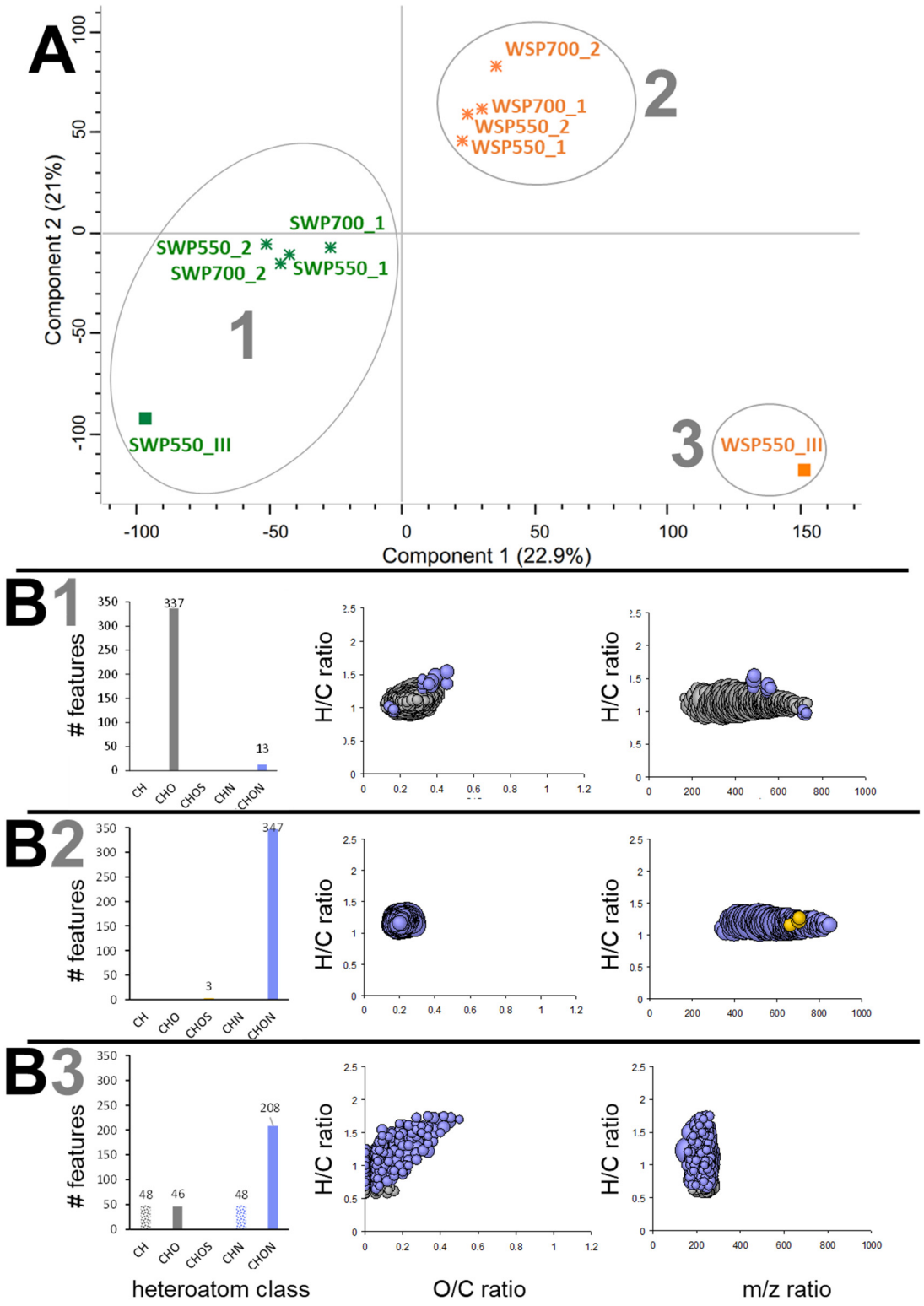

Figure 4. (**A**) Principal component analysis (PCA) score plot of all m/z features from bio-oils measured by APPI (+) FTICR MS. Wheat straw pellets-derived bio-oils in orange, softwood pellets bio-oils in green, small-scale unit bio-oils highlighted by a star and pilot-scale bio-oils by a full square. (**B**) Two hundred features specific to group 1, 2 and 3 observed in panel (**A**) were extracted and represented as (from left to right) bar chart according to their heteroatom classes, van Krevelen diagram (O/C vs. H/C) and m/z vs. H/C-ratios. The bubble size is relative to peak intensity.

As suggested previously, there is no ideal ionization mode for the analysis of pyrolysis liquids [19]. Both the detection and ionization modes are complementary and pyrolysis liquids should be analysed via different modes to get a full picture of the compounds present.

3.3. Effect of Pyrolysis Unit on the Liquid Composition

To compare the effect of mode of operation and scale of pyrolysis unit on the pyrolysis liquid composition principal component analyses (PCA) of data from ESI (+), ESI (−), and APPI (+) were performed (Figure 2A, Figure 3A, Figure 4A). In the PCA score plots the samples clearly cluster based on their feedstock. In addition, the molecular composition of the WSP-samples derived bio-oils is influenced by the pyrolysis unit design.

In the SWP-derived liquids, there is no spatial distinction of Stage I vs. Stage III samples in the PCA plots based on ESI (−) and ESI (+) modes (Figures 2A and 3A). The variability of the replicates produced under the same conditions and at different temperatures is similar to the variability of the samples produced in different pyrolysis units. This suggests the composition of the pyrolysis liquids derived primarily from polar lipids, carbohydrates and pyrolytic lignin are comparable between pyrolysis units of different scales. In APPI (+) there is some spatial distinction in the PCA plot (Figure 4A). The oxygen atom count distributions for the CxHyOz assignments obtained in ESI (+/−) and APPI (+) do not demonstrate differences with pyrolysis unit size (Figure S1). Though there is a slightly narrower distribution in APPI (+) for the sample produced in the Stage III unit. Thus, scale of the unit has a minor influence on the bio-oil molecular composition of SWP.

There is a much more pronounced effect of pyrolysis unit design in the WSP-derived bio-oils demonstrated in Figures 2–4. In all three analysis modes, WSP 550 produced in the Stage III unit does not cluster with the samples from the Stage I unit. A better insight into the molecular differences was given by extracting and plotting features specific to each cluster. In ESI (−) mode, O/C and H/C ratios were lower in the pyrolysis liquids produced in the continuous unit compared to samples from the batch unit (van Krevelen diagrams Figure 2(B2) vs. Figure 2(B3)). This indicates fewer oxygen species and a higher degree of unsaturation in the Stage III bio-oil. They also extent a narrower and smaller mass range (m/z 150–250) than the WSP samples produced in the batch unit (m/z 200–500). In positive ESI and APPI confirmed these results; the Stage I samples covered a broader mass range (m/z 200–800) than the Stage III bio-oil (Figure 3(B2,B3); Figure 4(B2,B3)). In addition, a higher diversity of compounds with different H/C and O/C ratios was detected. In ESI (−) and APPI (+) the CxHyOz distribution for the Stage III samples, according to the oxygen atom count, is narrower and shifted to lower values compared to the Stage I samples (Figure S2A,C).

The discrepancy in molecular composition of bio-oils produced in different pyrolysis units were particularly apparent in ESI (−) and APPI (+) mode, which are both more prone to detect pyrolytic lignin than sugar derivatives [19] suggesting that the type of pyrolysis unit mainly affected the conversion of lignin derived compounds. Overall, pyrolysis of WSP in the Stage III unit resulted in bio-oils with lower molecular diversity and lower and narrower mass range than bio-oils produced in the small-scale unit. The species formed in the Stage III unit are characterized by lower O/C and H/C ratios.

4. Discussion

We have previously shown that the pyrolysis units of different scale and modes described here produce biochars of similar quality in terms of key physicochemical properties, the volatile matter content (VM) and the fixed carbon content (FC) [25]. A higher FC content (FC on dry-ash-free = 1 − VM) is a sign of high biochar stability as a consequence of loss of functional groups and increasing degree of aromatization [30]. The FC content is a function of the thermal history of the biochar and reflects the primary thermo-chemical transformation reactions that also result in the formation of pyrolysis liquids. Therefore,

it is surprising that the FC/VM content is not statistically different in biochars from the continuous and batch pyrolysis unit [25], but the pyrolysis liquid composition is.

Boroson et al. (1989) demonstrated that otherwise stable pyrolysis vapours reacted and transformed in the presence of fresh wood char [42]. They further reported that only a part of the vapour fraction reacts with the char. This fraction is mostly lignin-derived, contains oxygen and is aromatic. Most of the difference in liquid composition as a result of the type of pyrolysis unit in our study can also be related to compounds that are lignin-derived.

Secondary solid-vapour reactions, mostly catalysed by minerals in the biomass/char but also the char itself [43], crack vapours of the primary products which are first converted into light hydrocarbons and oxygen-containing hydrocarbons, then further to aromatic tars and non-condensable gases (H_2, CO, CO_2 and H_2O) [44]. Only some of these pathways produce secondary char. A preference for vapour-based secondary reactions as also demonstrated in Zhang et al. [43] where the biochar yield stayed constant but the gas yield increased at the expense of the liquid yield could explain why the biochar were similar, but the liquid composition differed.

The Stage III is a continuous unit where the vapours travel along the shaft, so they have a longer residence time in the heated zone enabling further secondary reactions with the hot char in the reactor. These increasing secondary reactions in the rotary kiln resulted in a substantial decrease in pyrolysis liquid yield (Table 1) with a smaller increase in biochar yield. Comparing a larger data set of the biochars studied here, this biochar yield increase was not confirmed [25]. This further indicates that vapour cracking mainly resulted in the transformation of pyrolysis liquids into non-condensable gases as typical for catalytically mediated vapour reactions [45].

Reactions of the vapours with the char (and ash within) take place in the rotary kilns for a longer period of time compared to the batch unit. This results in dehydration, removal of oxygen and the release as H_2O, CO_2 and CO [16]. Such continuing catalytic decomposition reactions are responsible for the increase of the unsaturation degree and decrease of the oxygen amount per compound as observed in the Stage III bio-oils. These compounds are of lower molecular weight (Figure 2B, Figure 3B, Figure 4B), which increases the suitability of bio-oils for upgrading to fuels [46].

While the solid residence time at the highest treatment temperature is different between the two feedstocks (Table 1) due to slightly different sizes and densities of the pellets (Table 1), the vapour residence time is similar as the vapours on both occasions travel the same distance along the shaft of the kiln. Yet, WSP contains a higher mineral/ash content (6.44%) compared to SWP (~1% ash), which could explain the different behaviour of the feedstocks. Catalysts for pyrolysis vapour upgrading typically have a high micro/mesoporosity (e.g., zeolite or aluminosilicates), a balance of Lewis acid and basic sites and contain metal oxides [23,45,47,48]. They mainly deoxygenate the vapours and can result in extra char (coke) formation, yet depending on catalyst this formation of pyrolysis solids can be minimal [45,47,48].

Alkali and alkali earth metals, such as Mg and Na have been used as catalysts in combination with highly porous materials, such as zeolite [47,49,50]. Wheat straw (biochar) contains significant amounts of alkali and earth alkaline metals [51], and the biochar provides porosity. Recently, Zhang et al. (2020) demonstrated the potential for catalytic vapour cracking by both biochar and biochar-inherent alkali and earth alkaline metals and subsequent changes in the pyrolysis liquid composition [43]. This catalytic system might be less efficient and selective compared to an optimised external catalytic system. Yet, allowing for longer contact of vapours with the biochar at elevated temperatures in the continuous pyrolysis unit resulted in changes in the pyrolysis liquid composition, as also demonstrated previously [46].

Here, we show that this effect is a function of pyrolysis unit design and feedstock composition. It demonstrates that it is possible to improve the pyrolysis system even without external catalyst addition just by matching the pyrolysis unit design to the feed-

stock properties, in particular the mineral levels and composition. Here we used pelleted biomass for easier comparison of the behaviour of the two materials. The higher surface area of unpelleted wheat straw will likely further catalyse the cracking of pyrolysis vapours. The pyrolysis liquid composition and proportions of pyrolysis fractions could likely be optimised further by doping the feedstock with alkaline and earth alkaline metals as we have previously demonstrated for the stable carbon content in biochar [31,34,52]. This could enable the design of a pyrolysis system with maximum stable carbon content in the biochar (carbon retention) and high-quality pyrolysis liquids that could be used as fuel without or reduced need for further refinements.

5. Conclusions

This work provides important new insights into the effect of different pyrolysis mode (continuous vs. batch) and scale of operation on pyrolysis liquid composition, which, we previously demonstrated, did not significantly alter key characteristics in pyrolysis solids (biochar). The pyrolysis of softwood with mineral contents of only ~1% produced bio-oils of comparable composition in both pyrolysis units, while the molecular composition of bio-oils from wheat straw with a mineral content of ~6.5% clearly depends on the mode of operation of the pyrolysis unit. Consequently, it appears that the interaction of the nature of the feedstock and the pyrolysis unit drives the molecular composition of bio-oils. The pyrolysis liquids of wheat straw produced in the continuous unit contained compounds with lower oxygen content, higher degree of unsaturation and a higher proportion of lower molecular weight compounds. We hypothesise that this is a result of the longer travel distance of pyrolysis vapours in the heated zone in the continuous unit encouraging further secondary reactions that increase catalytic vapour cracking. This was likely pronounced in wheat straw compared to softwood due to the higher mineral/ash content in wheat straw and hence, a higher degree of catalytic reactions. To produce biofuels from straw materials, it could be beneficial to use continuous units with a long reactor shaft to maximise vapour residence time. This could optimise the process for co-production of biochar and bio-oil fuel in a low-cost and easily adaptable manner.

Supplementary Materials: The following are available online at https://www.mdpi.com/1996-1073/14/1/9/s1, Comparison of pyrolysis liquids from continuous and batch biochar production—Influence of feedstock evidenced by FTICR-MS.

Author Contributions: Conceptualization, W.B., J.H., V.C., C.L.M., F.A. and O.M.; formal analysis, J.H. and J.P.; funding acquisition, J.H.; investigation, J.H.; methodology, J.H. and C.L.M.; project administration, W.B. and J.H.; resources, C.L.M.; supervision, V.C., F.A. and O.M.; visualization, W.B., J.H. and J.P.; writing—original draft, W.B.; writing—review and editing, J.H., J.P., V.C., C.L.M., F.A. and O.M. All authors have read and agreed to the published version of the manuscript.

Funding: This research was funded by European COST Action 1306 "Lignoval".

Acknowledgments: The authors would like to thank the European COST Action 1306 "Lignoval" for its financial support that enabled the collaboration between the LCP-A2MC, Université de Lorraine and the UK Biochar Research Centre.

Conflicts of Interest: The authors declare no conflict of interest.

References

1. European Commission. *Circular Economy Action Plan—for a Cleaner and More Competitive Europe*; European Commission: Brussels, Belgium, 2020.
2. Zhu, J.; Fan, C.; Shi, H.; Shi, L. Efforts for a circular economy in China: A comprehensive review of policies. *J. Ind. Ecol.* **2019**, *23*, 110–118. [CrossRef]
3. State and Territory Governments; The Australian Local Government. *National Waste Policy—Less Waste, More Resources 2018*; 2018. Available online: https://www.environment.gov.au/system/files/resources/d523f4e9-d958-466b-9fd1-3b7d6283f006/files/national-waste-policy-2018.pdf (accessed on 21 December 2020).

4. Webb, J.; Hutchings, N.; Amon, B. 3.F Field burning of agricultural wastes. In *EMEP/EEA Emission Inventory Guidebook 2013*; 2013; pp. 1–14. Available online: https://www.google.com.hk/url?sa=t&rct=j&q=&esrc=s&source=web&cd=&cad=rja&uact=8&ved=2ahUKEwi74t3WyeDtAhVV62EKHUIjCU8QFjAAegQIAxAC&url=https%3A%2F%2Fwww.eea.europa.eu%2Fds_resolveuid%2FMWU9XE0TKP&usg=AOvVaw2AVcHTOaVo97k5aMQSnuWO (accessed on 21 December 2020).
5. Demirbas, A. Pyrolysis of ground beech wood in irregular heating rate conditions. *J. Anal. Appl. Pyrolysis* **2005**, *73*, 39–43. [CrossRef]
6. Bridgwater, A.V.; Peacocke, G.V.C. Fast pyrolysis processes for biomass. *Renew. Sustain. Energy Rev.* **2000**, *4*, 1–73. [CrossRef]
7. Boateng, A.A.; Garcia-Perez, M.; Mašek, O.; Brown, R.; del Campo, B. Chapter 4: Biochar production technology. In *Biochar for Environmental Management: Science and Technology and Implementation*, 2nd ed.; Earthscan Ltd.: London, UK, 2015; pp. 53–66.
8. Crombie, K.; Mašek, O. Pyrolysis biochar systems, balance between bioenergy and carbon sequestration. *GCB Bioenergy* **2015**, *7*, 349–361. [CrossRef]
9. Lehmann, J.; Joseph, S. Chapter 1: Biochar for environmental managment: An introduction. In *Biochar for Environmental Management: Science and Technology and Implementation*, 2nd ed.; Earthscan Ltd.: London, UK, 2015; pp. 1–13.
10. Brown, R.; del Campo, B.; Boateng, A.A.; Garcia-Perez, M.; Mašek, O. Chapter 3: Fundamentals of biochar production. In *Biochar for Environmental Management: Science and Technology and Implementation*, 2nd ed.; Earthscan Ltd.: London, UK, 2015; pp. 39–61.
11. Smith, P. Soil carbon sequestration and biochar as negative emission technologies. *Glob. Chang. Biol.* **2016**, *22*, 1315–1324. [CrossRef]
12. Liu, W.; Jiang, H.; Yu, H. Emerging applications of biochar-based materials for energy storage and conversion. *Energy Environ. Sci.* **2019**. [CrossRef]
13. Edeh, I.G.; Mašek, O.; Buss, W. A meta-analysis on biochar's effects on soil water properties–New insights and future research challenges. *Sci. Total Environ.* **2020**, *714*. [CrossRef]
14. Buss, W.; Kammann, C.; Koyro, H.-W. Biochar reduces copper toxicity in Chenopodium quinoa Willd in a sandy soil. *J. Environ. Qual.* **2012**, *41*, 1157–1165. [CrossRef]
15. Crombie, K.; Mašek, O. Investigating the potential for a self-sustaining slow pyrolysis system under varying operating conditions. *Bioresour. Technol.* **2014**, *162*, 148–156. [CrossRef]
16. Zhang, Q.; Chang, J.; Wang, T.; Xu, Y. Review of biomass pyrolysis oil properties and upgrading research. *Energy Convers. Manag.* **2007**, *48*, 87–92. [CrossRef]
17. Staš, M.; Chudoba, J.; Kubička, D.; Blažek, J.; Pospíšil, M. Petroleomic characterization of Pyrolysis bio-oils: A review. *Energy Fuels* **2017**, *31*, 10283–10299. [CrossRef]
18. Harman-Ware, A.E.; Ferrell, J.R. Methods and challenges in the determination of molecular weight metrics of bio-oils. *Energy Fuels* **2018**, *32*, 8905–8920. [CrossRef]
19. Hertzog, J.; Carré, V.; Le Brech, Y.; Mackay, C.L.; Dufour, A.; Mašek, O.; Aubriet, F. Combination of electrospray ionization, atmospheric pressure photoionization and laser desorption ionization Fourier transform ion cyclotronic resonance mass spectrometry for the investigation of complex mixtures—Application to the petroleomic analysis. *Anal. Chim. Acta* **2017**, *969*, 26–34. [CrossRef] [PubMed]
20. Elliott, D.C.; Schiefelbein, G.F. Liquid hzdrocarbon fuels from biomass. *Am. Chem. Soc. Div. Fuel Chem. Prepr.* **1989**, *34*, 1160–1166.
21. Czernik, S.; Bridgwater, A.V. Overview of applications of biomass fast pyrolysis oil. *Energy Fuels* **2004**, *18*, 590–598. [CrossRef]
22. Hertzog, J.; Carre, V.; Aubriet, F. Contribution of Fourier transform mass spectrometry to bio-oil study. In *Fundamentals and Applications of Fourier Transform Mass Spectrometry*; Elsevier: Amsterdam, The Netherlands, 2019; pp. 679–733. ISBN 9780128140130.
23. Hertzog, J.; Carré, V.; Jia, L.; Mackay, C.L.; Pinard, L.; Dufour, A.; Mašek, O.; Aubriet, F. Catalytic fast pyrolysis of biomass over microporous and hierarchical zeolites: Characterization of heavy products. *ACS Sustain. Chem. Eng.* **2018**, *6*, 4717–4728. [CrossRef]
24. Hertzog, J.; Carré, V.; Le Brech, Y.; Dufour, A.; Aubriet, F. Toward controlled ionization conditions for ESI-FT-ICR-MS analysis of bio-oils from lignocellulosic material. *Energy Fuels* **2016**, *30*, 5729–5739. [CrossRef]
25. Mašek, O.; Buss, W.; Roy-Poirier, A.; Lowe, W.; Peters, C.; Brownsort, P.; Mignard, D.; Pritchard, C.; Sohi, S. Consistency of biochar properties over time and production scales: A characterisation of standard materials - Available online 24 February 2018. *J. Anal. Appl. Pyrolysis* **2018**, *132*, 200–210. [CrossRef]
26. Crombie, K.; Mašek, O.; Sohi, S.P.; Brownsort, P.; Cross, A. The effect of pyrolysis conditions on biochar stability as determined by three methods. *GCB Bioenergy* **2013**, *5*, 122–131. [CrossRef]
27. Roullier-Gall, C.; Boutegrabet, L.; Gougeon, R.D.; Schmitt-Kopplin, P. A grape and wine chemodiversity comparison of different appellations in Burgundy: Vintage vs terroir effects. *Food Chem.* **2014**, *152*, 100–107. [CrossRef]
28. Miettinen, I.; Mäkinen, M.; Vilppo, T.; Jänis, J. Compositional characterization of phase-separated pine wood slow pyrolysis oil by negative-ion electrospray ionization fourier transform ion cyclotron resonance mass spectrometry. *Energy Fuels* **2015**, *29*, 1758–1765. [CrossRef]
29. Ronsse, F.; van Hecke, S.; Dickinson, D.; Prins, W. Production and characterization of slow pyrolysis biochar: Influence of feedstock type and pyrolysis conditions. *GCB Bioenergy* **2013**, *5*, 104–115. [CrossRef]
30. Antal, M.J.; Grønli, M. The art, science, and technology of charcoal production. *Ind. Eng. Chem. Res.* **2003**, *42*, 1619–1640. [CrossRef]

31. Buss, W.; Jansson, S.; Wurzer, C.; Mašek, O. Synergies between BECCS and biochar-maximizing carbon sequestration potential by recycling wood ash-accepted. *ACS Sustain. Chem. Eng.* **2019**. [CrossRef]
32. Fuentes, M.E.; Nowakowski, F.J.; Kubacki, M.L.; Cove, J.M.; Bridgeman, T.G.; Jones, J.M. A survey of the influence of biomass mineral matter in the thermochemical conversion of short rotation willow coppice. *J. Energy Inst.* **2008**, *81*, 234–241. [CrossRef]
33. Nowakowski, D.J.; Jones, J.M.; Brydson, R.M.D.; Ross, A.B. Potassium catalysis in the pyrolysis behaviour of short rotation willow coppice. *Fuel* **2007**, *86*, 2389–2402. [CrossRef]
34. Mašek, O.; Buss, W.; Brownsort, P.; Rovere, M.; Alberto, T. Potassium doping increases biochar carbon sequestration potential by 45 %, facilitating decoupling of carbon sequestration from soil improvement. *Sci. Rep.* **2019**, *9*, 5514. [CrossRef]
35. Kujawinski, E.B. Electrospray ionization fourier transform Ion Cyclotron resonance mass spectrometry (ESI FT-ICR MS): Characterization of complex environmental mixtures. *Environ. Forensics* **2002**, *3*, 207–216. [CrossRef]
36. Cole, D.P.; Smith, E.A.; Dalluge, D.; Wilson, D.M.; Heaton, E.A.; Brown, R.C.; Lee, Y.J. Molecular characterization of nitrogen-containing species in switchgrass bio-oils at various harvest times. *Fuel* **2013**, *111*, 718–726. [CrossRef]
37. Jarvis, J.M.; Page-dumroese, D.S.; Anderson, N.M.; Corilo, Y.; Rodgers, R.P. Characterization of fast pyrolysis products generated from several Western USA woody species. *Energy Fuels* **2014**, *28*, 6438–6446. [CrossRef]
38. O'Neill, M.A.; Eberhard, S.; Albersheim, P.; Darvill, A.G. Requirement of borate cross-linking of cell wall rhamnogalacturonan II for Arabidopsis growth. *Science* **2001**, *294*, 846–849. [CrossRef] [PubMed]
39. Pappin, R.; Kiefel, M.J.; Houston, T.A. Boron-Carbohydrate interactions. In *Carbohydrates—Comprehensive Studies on Glycobiology and Glycotechnology*; Chang, C.-F., Ed.; IntechOpen: London, UK, 2011.
40. Penn, S.G.; Hu, H.; Brown, P.H.; Lebrilla, C.B. Direct analysis of sugar alcohol borate complexes in plant extracts by matrix-assisted laser desorption/ionization fourier transform mass spectrometry. *Anal. Chem.* **1997**, *69*, 2471–2477. [CrossRef]
41. Gaspar, A.; Lucio, M.; Harir, M.; Schmitt-Kopplin, P. Targeted and non-targeted boron complex formation followed by electrospray Fourier transform ion cyclotron mass spectrometry: A novel approach for identifying boron esters with natural organic matter. *Eur. J. Mass Spectrom.* **2011**, *17*, 113–123. [CrossRef] [PubMed]
42. Boroson, M.L.; Howard, J.B.; Longwell, J.P.; Peters, W.A. Heterogeneous cracking of wood pyrolysis tars over fresh wood char surfaces. *Energy Fuels* **1989**, *3*, 735–740. [CrossRef]
43. Zhang, Y.; Zhang, J.; Chen, F.; Ma, H.; Chen, D. Influence of biochar with loaded metal salts on the cracking of pyrolysis volatiles from corn straw. *Energy Sources Part A Recover. Util. Environ. Eff.* **2020**, 1–10. [CrossRef]
44. Evans, R.J.; Milne, T.A. Molecular characterization of the pyrolysis of biomass. 2. Applications. *Energy Fuels* **1987**, *1*, 311–319. [CrossRef]
45. Yaman, E.; Yargic, A.S.; Ozbay, N.; Uzun, B.B.; Kalogiannis, K.G.; Stefanidis, S.D.; Pachatouridou, E.P.; Iliopoulou, E.F.; Lappas, A.A. Catalytic upgrading of pyrolysis vapours: Effect of catalyst support and metal type on phenolic content of bio-oil. *J. Clean. Prod.* **2018**, *185*, 52–61. [CrossRef]
46. Huang, Y.; Kudo, S.; Mašek, O.; Norinaga, K.; Hayashi, J.I. Simultaneous maximization of the char yield and volatility of oil from biomass pyrolysis. *Energy Fuels* **2013**, *27*, 247–254. [CrossRef]
47. Iliopoulou, E.F.; Triantafyllidis, K.S.; Lappas, A.A. Overview of catalytic upgrading of biomass pyrolysis vapors toward the production of fuels and high-value chemicals. *Wiley Interdiscip. Rev. Energy Environ.* **2019**, *8*, 1–29. [CrossRef]
48. Balasundram, V.; Zaman, K.K.; Ibrahim, N.; Kasmani, R.M.; Isha, R.; Hamid, M.K.A.; Hasbullah, H. In situ catalytic upgrading of oxygenated pyrolysis vapours from pyrolysis of sugarcane bagasse over metal oxides loaded HZSM-5. *Biomass Convers. Biorefin.* **2020**, *5*. [CrossRef]
49. Nguyen, T.S.; Zabeti, M.; Lefferts, L.; Brem, G.; Seshan, K. Catalytic upgrading of biomass pyrolysis vapours using faujasite zeolite catalysts. *Biomass Bioenergy* **2013**, *48*, 100–110. [CrossRef]
50. Stefanidis, S.D.; Kalogiannis, K.G.; Iliopoulou, E.F.; Lappas, A.A.; Pilavachi, P.A. In-situ upgrading of biomass pyrolysis vapors: Catalyst screening on a fixed bed reactor. *Bioresour. Technol.* **2011**, *102*, 8261–8267. [CrossRef] [PubMed]
51. Buss, W.; Graham, M.C.; Shepherd, J.G.; Mašek, O. Suitability of marginal biomass-derived biochars for soil amendment. *Sci. Total Environ.* **2016**, *547*, 314–322. [CrossRef]
52. Buss, W.; Bogush, A.; Ignatyev, K. Unlocking the fertilizer potential of waste-derived biochar. *ACS Sustain. Chem. Eng.* **2020**, *8*, 12295–12303. [CrossRef]